

# Mathematical Modeling of a Unicycle Robot and Use of Advanced Control Methodologies for Multi-Paths Tracking Taking into Account Surface Friction Factors

Mohamed Abdelhakim Basal <sup>1\*</sup>, Mohammed Fadhil Ahmed <sup>2</sup>

<sup>1</sup> Faculty of Engineering, Menoufia University, Egypt

<sup>2</sup> Department of Computer Technical Engineering, Al-Qalam University College, Kirkuk 36001, Iraq

Email: <sup>1</sup> mohamedabdelhikeem@yahoo.com, <sup>2</sup> mohammed.ahmed@alqalam.edu.iq

\*Corresponding Author

**Abstract**—The research aims to design robust controllers that achieve the stability of a single-wheeled robot under the presence of friction factors and to track different parameters to verify robust stability. This paper presents a new study of the unicycle robot system that is controlled using advanced control methodologies. The paper aims to improve the work of the unicycle robot system, due to its effective impact on improving the performance of driving the robot, which is reflected in the smoothness of the vehicle speed change, ensuring the stability of the robot and the safety of the investor in the uncertain work environment. The main goal is to achieve high dynamic performance for the unicycle robot system. The studied system is non-linear and is subject to the restrictions of the friction factor change with the speed change of the unicycle robot. What increases the difficulty of controlling this type of control system is the uncertainty of some parameters of the control system, such as friction factors. In this paper, two advanced control methodologies were proposed: the optimal controller and the optimal parametric controller. The research results showed that both the optimal and optimal parametric controllers succeeded in achieving stability despite the uncertainty of the parameters and multiple friction factors, but with a relative superiority of the optimal parametric controller. Previous research has discussed many controllers such as classical and advanced controllers such as sliding control and fuzzy control, but it has not previously dealt with the optimal parametric controller that will be discussed in this research.

**Keywords**—Unicycle Robot; Optimal Parametric Controller; Optimal Integral Controller; Advanced Control.

## I. INTRODUCTION

The importance of the paper is that the unicycle robot system can be widely used in large facilities, Such as hospitals, stadiums and large factories. where this can be done using the unicycle robot. The appropriate controller design to control the operation of the control system, taking into account the uncertainty of the control system parameters and their real modeling, will be reflected in the safe driving of vehicles, which leads to the comfort of the investor, whether he is a doctor, athlete, engineer or cleaner, and will be reflected in improving the performance and stability of the control system [1].

The single-wheeled robot system is a difficult problem because it is an unstable and highly vibrating system, and it

is considered a system with high uncertainties. The problem is further complicated by the friction factors that arise when the robot moves on surfaces of different roughness, so the designed controller must face these complex issues.

The emergence of the COVID-19 coronavirus has contributed to increased interest in autonomous robots to serve humans without direct interaction between them. as the importance of providing service in hospitals, restaurants and other tourist places has increased remotely, in order to reduce direct interaction between humans to reduce infections. Among these robots that have been developed is the unicycle robot due to its ease of driving and control.

Many papers in recent years have addressed the subject of controlling the unicycle robot system and employing this paper in its application to various robots to serve humans in a way that ensures efficiency in driving these robots to achieve the desired response and tracking various reference paths. This requires that this system has a rapid response to the change in the friction factor that negatively affects the performance of the robot and its driving and may lead to unexpected accidents. Therefore, to avoid these accidents, work was done in this paper to design advanced controllers to ensure the best performance and fastest response for the unicycle robot system. What increases the difficulty of control is the presence of uncertainty in the dynamic and kinetic parameters such as the change in the friction factor of the robot as a result of rust and dirt that can accumulate over time [2].

This paper discusses the design of advanced controllers, including the optimal controller and the optimal parametric controller, to obtain high dynamic performance and resistance to uncertainties affecting the unicycle robot system. In this paper, the studied control system was simulated using the MATLAB/SIMULINK environment, and the results showed high performance of the control system.

The optimal controller will be designed for a nominal parameter control system. It does not take uncertainty into account, while the optimal parametric controller takes uncertainty into account, by representing the system in the



form of an affine where uncertainty is taken into account in the two matrices ( $L$ ,  $N$ ) as we will see later.

The paper contributed to solving the issue of tracking different paths with the presence of friction factors according to the horizontal and vertical movement directions.

## II. IMPORTANCE OF THE PAPER

The importance of the paper is that the unicycle robot is used in many vital places, where a quick response is required due to the danger and importance of being present in the shortest possible time to save a patient's life or to treat the injured in dangerous workplaces such as large factories where it is difficult for ambulances to enter, so the unicycle robot is used as an alternative to achieve this goal, and the design of the appropriate controller to control the operation of the control system, taking into account the uncertainty of the control system parameters and their real modeling, will be reflected in the safe driving of the unicycle robot, which leads to human comfort.

Despite these promising applications, controlling a single-wheeled robot presents challenges, especially in environments with dynamic conditions such as variable friction or uncertainty in control parameters.

The reason for the importance of the single-wheeled robot is its low mechanical complexity, as it relies on one wheel and therefore requires only one motor, as well as its low cost compared to robots that require four wheels, as well as its small size.

## III. REFERENCE STUDIES

Many studies dealt with the design of controllers for a unicycle robot. Among these studies we:

### A. First Paper

In the paper [1] (2024) "An Integral Sliding-Mode-based Robust Interval Predictive Control for Perturbed Unicycle Mobile Robots", the researchers: "Hector Ríos, Manuel Mera, Tarek Raïssi, Denis Efimov", used the robust control methodology for trajectory tracking in single-disturbance unicycle mobile robots, where the proposed strategy included the design of a robust control law. It is based on the integral sliding mode control (ISMC) approach combined with a state feedback controller based on time-lapse prediction and a model predictive control (MPC) scheme. The robust controller handles some perturbations in the kinematic model, and with state and input constraints associated with the constraints of the workspace and saturated actuators respectively. The proposed approach ensures exponential convergence to zero of the tracking error, and the tracking has been verified through simulation using MATLAB.

### B. Second Paper

In the paper [2] (2023) "Autonomous unicycle: modeling, dynamics, and control", the researchers "Xincheng Cao, Dang Cong Bui, Dénes Takács, Gábor Orosz," derived the kinematic equations of the unicycle robot system, based on the AP-Pellian method, for which the control system is represented by state equations in their minimum form. The PD controller was designed to achieve stability with 3 rotational torques in order to control the unicycle robot from

the fixed position and then follow the specified path. The control system was numerically simulated, and the results were good.

### C. Third Paper

In the paper [3] (2019) "Self-triggered MPC for trajectory tracking of unicycle-type robots with external disturbance", researchers "Qun Cao, Zhongqi Sun, Yuanqing Xia, Li Dai" designed the controller based on the self-triggered predictive controller (MPC) methodology for the unicycle-type robot system, with a constraint on the control beam and taking into account limited external disturbances, where the design was based on the Lyapunov function and then the stability of the closed-loop system was improved, and the simulation results showed the effectiveness of the proposed algorithm.

This paragraph introduces the latest research on the uni-wheeled robot and the controllers used to organize its operation.

## IV. PROBLEM STATEMENT

The dynamic model of the unicycle robot system taking into account the uncertainty of friction factors will be derived below.

Despite these promising applications, controlling a single-wheeled robot presents challenges, especially in environments with dynamic conditions such as variable friction or uncertainty in control parameters.

### A. Modeling of the Unicycle Robot [1]-[32]:

Fig. 1 shows the basic components of a single-wheeled robot:



Fig. 1. The basic components of a unicycle robot

These parts are:

- The arm, which works similarly to an inverted pendulum.
- The wheel.
- DC motors, where there are two motors: the first to move the wheel and the second to return the arm so that it is vertical. Fig. 2 also shows the detailed structure with the coordinates for both the arm and the wheel.

The working principle initially depends on the movement of the wheel by the first DC motor, and then the second DC

motor will be operated, which tries to keep the arm vertical without falling, so the control sentence can be described by two coordinate sentences, which are:

- The first coordinate set to describe the arm, and the center of this set will be the center of gravity of the arm, and in this case, the movement of the arm will create two angles, which are  $\alpha_1(t)$ , which is the angle between the axis of the arm and the vertical line passing through the axis of the wheel, and  $\alpha_2(t)$ , the angle between the axis of the arm and the axis perpendicular to the plane of the wheel.

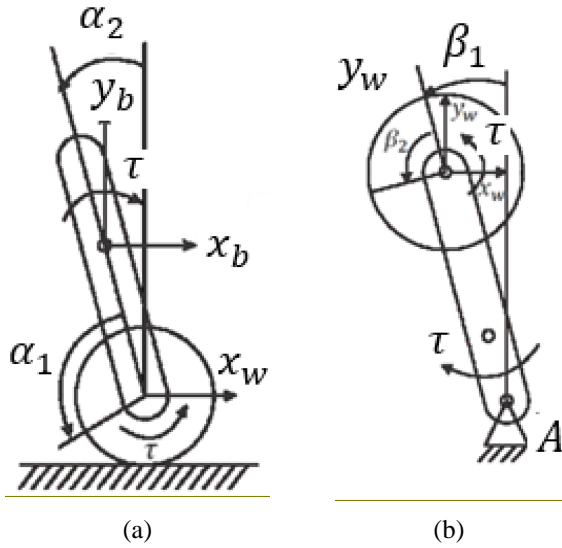


Fig. 2. Detailed structure of the unicycle robot assembly with coordinates

- The second coordinate system to describe the wheel, and the center of this system is the center point of the wheel, in this case, the movement of the wheel will create two angles, which are  $\beta_1(t)$ , which is the angle resulting from the rotation of the wheel relative to the plumb line passing through point (A), and  $\beta_2(t)$ , the angle resulting from the rotation of the wheel and the axis perpendicular to the plane of the wheel.

To determine the mathematical model of the unicycle robot, the following Lagrange equation can be used [52]:

$$\frac{d}{dt} \left( \frac{\partial L}{\partial \dot{q}_r} \right) - \frac{\partial L}{\partial q_r} = \tau_r \quad (1)$$

Where,  $L$  is the Lagrange function.  $q_r$  is the coordinate angles of the unicycle.  $\tau_r$  is the torque applied to the unicycle.

The Lagrange energy function is given by:

$$L = E_K - E_P \quad (2)$$

Where,  $E_K$  is the kinetic energy of the unicycle robot.  $E_P$  is the potential energy of the unicycle robot.

To find the mathematical model of the unicycle robot, the robot assembly can be divided into two separate parts and the mathematical model for each part can be found separately as follows:

### B. Mathematical Model of the Robot Arm

It represents an inverted pendulum, and according to Fig. 2(a), we notice that the robot arm has two degrees of freedom,

which are the angles  $\alpha_1(t), \alpha_2(t)$ . By applying the Lagrange relation to the angles  $\alpha_1(t), \alpha_2(t)$ , we obtain the following mathematical model that describes the robot arm:

$$(J_w + m_w r_{bt}^2 + m_{bt} r_{bt}^2) \ddot{\alpha}_1 + m_{bt} r_{bt} \cos(\alpha_2) \ddot{\alpha}_2 \\ - m_{bt} r_{bt} l_{bt} \sin(\alpha_2) \dot{\alpha}_2^2 + (\mu_f + \mu_a) \dot{\alpha}_1 - \mu_a \dot{\alpha}_2 = \tau_m \quad (3)$$

$$m_{bt} r_{bt} l_{bt} \cos(\alpha_2) \ddot{\alpha}_1 + (m_{bt} l_{bt}^2 + J_{bt}) \ddot{\alpha}_2 - \mu_a \dot{\alpha}_1 \\ + \mu_a \dot{\alpha}_2 - m_{bt} g l_{bt} \sin(\alpha_2) = -\tau_m \quad (4)$$

The parameters of the robot arm are shown in Table I.

TABLE I. ROBOT ARM PARAMETERS

Parameters	Description	Value
$J_w$	Moment of inertia of the wheel with respect to the center of the arm	0.000158 ( $kg \cdot m^2$ )
$m_w$	wheel mass	0.053 ( $m$ )
$r_{bt}$	Wheel radius	0.225 ( $kg$ )
$m_{bt}$	arm mass	1.586 ( $kg$ )
$l_{bt}$	The distance between the center of the wheel and the center of gravity of the arm	0.56 ( $m$ )
$\mu_f$	Wheel friction factor with the ground	[0, 1]
$\mu_a$	Wheel hub friction factor	[0, 1]
$g$	acceleration due to gravity	9.81 ( $\frac{m}{sec^2}$ )

### C. Mathematical Model of the Android Wheel

Representing a scene as a touch control system as a reaction to the robot arm in the opposite direction to the arm above the rocket arm vertically, and determining the Fig. 2(b) we notice that the Android wheel has two degrees of freedom, which are the angles  $\beta_1(t), \beta_2(t)$ . Which means the Lagrange relation on the angles  $\beta_1(t), \beta_2(t)$ . We get the following mathematical model that describes the robot wheel:

$$J \ddot{\beta}_1 + (\mu_{pr} + \mu_{rw}) \dot{\beta}_1 - \mu_{rw} \dot{\beta}_2 + mgl_1 \sin(\beta_1) \\ = -\tau_m \quad (5)$$

$$J_{2c} \ddot{\beta}_2 - \mu_{rw} \dot{\beta}_1 + \mu_{rw} \dot{\beta}_2 = \tau_m \quad (6)$$

The parameters of the robot wheel are shown in Table II.

TABLE II. ROBOT WHEEL PARAMETERS

Parameters	Description	Value
$J = J_p + m_w l_{1c}^2 + m_{bt} l_1^2$	torque of inertia of the wheel	1.66046 ( $kg \cdot m^2$ )
$J_p$	Moment of inertia of robot arm	0.0039 ( $kg \cdot m^2$ )
$l_{1c}$	robot arm length	0.56 ( $m$ )
$l_1$	Distance between center of wheel and point (A)	1.586 ( $kg$ )
$l_{bt}$	The distance between the center of the wheel and the center of gravity of the arm	0.56 ( $m$ )
$\mu_{pr}$	Arm friction factor with wheel	[0, 1]
$\mu_{rw}$	Wheel axle backlash friction factor	[0, 1]
$J_{2c}$	Moment of inertia of the wheel with respect to its center	0.00063 ( $kg \cdot m^2$ )

#### D. Mathematical Model of the Unicycle Robot

Approximating the trigonometric ratios in relations (3), (4) and (5) for small angles:

$$\begin{aligned}\sin(\beta_1) &\approx \beta_1, \cos(\beta_1) \approx 1 \\ \sin(\alpha_1) &\approx \alpha_1, \cos(\alpha_1) \approx 1\end{aligned}\quad (7)$$

The mathematical model of the unicycle robot after using the data given in Table I and Table II becomes as follows:

$$0.0052\ddot{\alpha}_1 + 0.0471\dot{\alpha}_2 - 0.0471\alpha_2\dot{\alpha}_2 + (\mu_f + \mu_a)\dot{\alpha}_1 - \mu_a\dot{\alpha}_2 = \tau_m \quad (8)$$

$$0.0471\ddot{\alpha}_1 + 0.6746\dot{\alpha}_2 - \mu_a\dot{\alpha}_1 + \mu_a\dot{\alpha}_2 - 8.7128\alpha_2 = -\tau_m \quad (9)$$

$$0.1772\ddot{\beta}_1 + (\mu_{pr} + \mu_{rw})\dot{\beta}_1 - \mu_{rw}\dot{\beta}_2 + 16.79472\beta_1 = -\tau_m \quad (10)$$

$$0.00063\ddot{\beta}_2 - \mu_{rw}\dot{\beta}_1 + \mu_{rw}\dot{\beta}_2 = \tau_m \quad (11)$$

In order to find the equations of state for the robot arm model we impose the following variables:

$$x_{p1} = \alpha_1, x_{p2} = \dot{\alpha}_1, x_{p3} = \alpha_2, x_{p4} = \dot{\alpha}_2 \quad (12)$$

In order to find the equations of state for the robot wheel model we impose the following variables:

$$x_{w1} = \beta_1, x_{w2} = \dot{\beta}_1, x_{w3} = \beta_2, x_{w4} = \dot{\beta}_2 \quad (13)$$

Then we get the equations of state for the robot arm according to the following formula:

$$\dot{x}_{p1}(t) = x_{p2}(t)$$

$$\begin{aligned}\dot{x}_{p2}(t) &= -9.0577x_{p4}(t) + 9.0577x_{p3}(t)x_{p4}^2 \\ &\quad - 192.3077(\mu_f + \mu_a)x_{p2} \\ &\quad + 192.3077\mu_a x_{p4} \\ &\quad + 192.3077\tau_m \\ \dot{x}_{p3}(t) &= x_{p4}(t) \\ \dot{x}_{p4}(t) &= (-12.7944 + 13.4268\mu_f \\ &\quad + 11.9444\mu_a)x_{p4}(t) \\ &\quad - 0.6324x_{p3}(t)x_{p4}^2 \\ &\quad + 1.4824x_{p2} + 12.9155x_{p3} \\ &\quad - 14.9091\tau_m\end{aligned}\quad (14)$$

The equations of state for the robot wheel are as follows:

$$\dot{x}_{w1}(t) = x_{w2}(t)$$

$$\begin{aligned}\dot{x}_{w2}(t) &= -5.6433(\mu_{pr} + \mu_{rw})x_{w2}(t) \\ &\quad + 5.6433x_{w4}(t) - 94.7754x_{w1} \\ &\quad - 5.6433\tau_m \\ \dot{x}_{w3}(t) &= x_{w4}(t) \\ \dot{x}_{w4}(t) &= 1587.3\mu_{rw}x_{w2}(t) - 1587.3\mu_{rw}x_{w4}(t) \\ &\quad + 1587.3\tau_m\end{aligned}\quad (15)$$

#### E. Block Diagram to Represent the Single-Wheel Robot System

Fig. 3 shows the Simulink diagram to represent the single-wheel robot system, in the open loop according to its

mathematical model represented by state equations (14) and (15)[5][6].

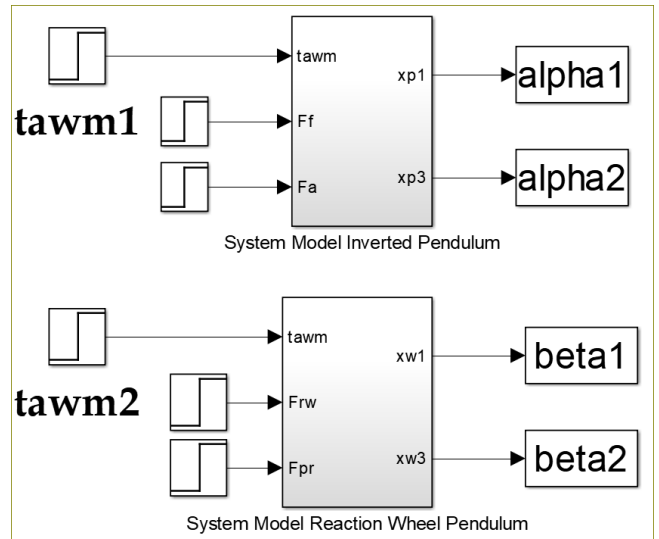


Fig. 3. Simulink diagram to represent the unicycle robot system in the open loop

#### F. Response of the Single-Wheel Robot in the Open Loop

By implementing the scheme shown in Fig. 3, we obtain the following responses, where the input signal is the torque signal generated by the DC motor, and the response is the angles of the robot arm ( $\alpha_1(t), \alpha_2(t)$ ) and the angles of the wheel ( $\beta_1(t), \beta_2(t)$ ).

- Response of the angle between the arm axis and the vertical line passing through the wheel axis  $\alpha_1(t)$ :

The angle  $\alpha_1(t)$  is called the swing angle of the robot arm around the vertical axis (Pitch Angle), and when applying the optimal controller to the nonlinear single-wheel robot system.

Fig. 4 shows the response of the angle between the arm axis and the vertical line passing through the wheel axis  $\alpha_1(t)$  for the nonlinear single-wheel robot system in the open loop:

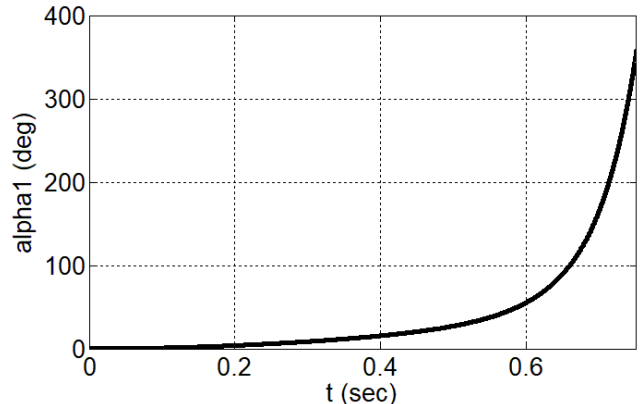


Fig. 4. Response of angle  $\alpha_1(t)$  of the nonlinear robot system in the open loop

- Roll Angle Response of Robot Arm  $\alpha_2(t)$ :

The angle  $\alpha_2(t)$  is called the angle of inclination of the robot arm relative to the vertical plane (Roll Angle), and when applying the optimal controller to the nonlinear single-wheel robot system.

Fig. 5 shows the response of the angle between the arm axis and the axis perpendicular to the wheel plane  $\alpha_2(t)$  for the nonlinear single-wheel robot system in the open loop:

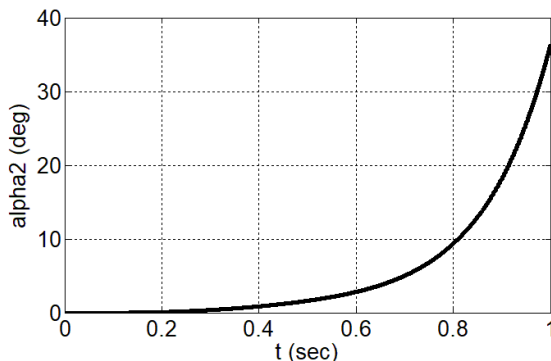


Fig. 5. Roll Angle Response of Robot Arm  $\alpha_2(t)$  of the nonlinear robot system in the open loop

- The response of the angle resulting from the rotation of the wheel relative to the vertical line passing through point (A)  $\beta_1(t)$ :

Fig. 6 shows the response of the angle resulting from the rotation of the wheel relative to the vertical line passing through point (A)  $\beta_1(t)$  for the nonlinear single-wheel robot system in the open loop:

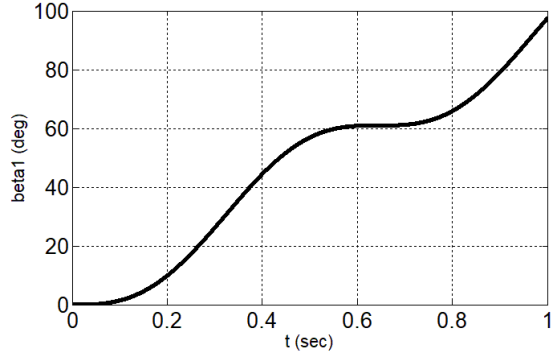


Fig. 6. Response of angle  $\beta_1(t)$  of the nonlinear robot system in the open loop

- Angle response resulting from the rotation of the wheel and the axis perpendicular to the wheel plane  $\beta_2(t)$ :

Fig. 7 shows the angle response resulting from the rotation of the wheel and the axis perpendicular to the wheel plane  $\beta_2(t)$ : for the nonlinear single-wheel robot system in the open loop:

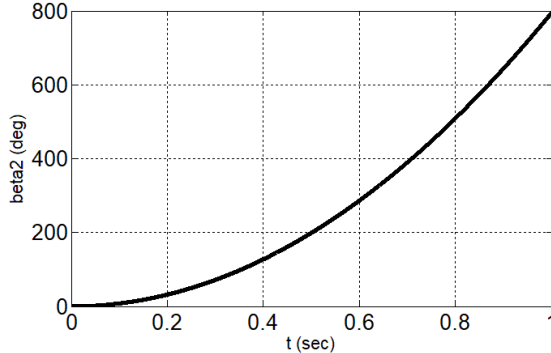


Fig. 7. Response of angle  $\beta_2(t)$ : of the nonlinear robot system in the open loop

From these responses shown in Fig. 4, Fig. 5, Fig. 6, and Fig. 7, we notice that the open-loop single-wheel robot system is unstable, and appropriate controllers must be designed that achieve strong stability when the single-wheel robot system parameters are uncertain.

In this paragraph, we identified the mechanical structure of the single-wheeled robot and its main parts, deduced its mathematical model using the Lagrange method, then found the state equations and represented them in the MATLAB environment, then found the responses to the unicycle robot system in the open loop.

## V. DESIGN OF THE OPTIMAL CONTROLLER [62]-[80]

Optimal controller is defined as the control vector design of a control system that minimizes the performance function to the lowest value, for the given eigenvalues of the control system.

Fig. 8 shows the general block diagram of the linear quadratic optimal controller:

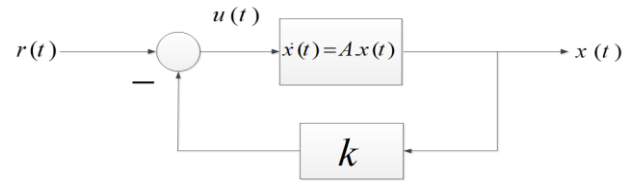


Fig. 8. Block diagram of the optimal control problem

The mathematical model of the control set based on the state variables is given by the following formula:

$$\begin{aligned} \dot{x}(t) &= A.x(t) + B.u(t) \\ y(t) &= C.x(t) \end{aligned} \quad (16)$$

According to Fig. 8, the control signal is given by the difference between the reference signal  $r(t)$  and the linear combination consisting of the components of the state vector:

$$u(t) = r(t) - kx(t) \quad (17)$$

where  $r(t)$  is the reference signal,  $k$  is the optimal control gain vector of dimension  $(n)$  and  $u(t)$  is the control vector that must be designed to minimize the following cost function:

$$J = \frac{1}{2} \int_0^{t_f} (x^T Q x + R u^2) dt \quad (18)$$

Both  $(Q, R)$  are positively defined symmetric matrices. The optimal control vector is given by:

$$u(t) = k_{optimal} \cdot x(t) \quad (19)$$

Where as the optimal control gain is:

$$k_{optimal} = -R^{-1} \cdot B^T \cdot P \quad (20)$$

Where  $(P)$  is the solution to the following Riccati algebraic equation:

$$P \cdot A + A^T \cdot P - P \cdot B \cdot R^{-1} \cdot B \cdot P + Q = 0 \quad (21)$$

Since the optimal quadratic controller is applied to the linear control system, the linear control system for the unicycle robot model was initially found based on Jacobi relations at the equilibrium point.

This paragraph explains the mechanism of designing the linear quadratic optimization controller.

## VI. LINEAR APPROXIMATION ACCORDING TO JACOBI [33]-[52]

Let the nonlinear control system be described by the following state equations:

$$\begin{aligned}\dot{x}(t) &= f(x(t), u(t)) \\ y(t) &= h(x(t), u(t))\end{aligned}\quad (22)$$

Where  $x(t)$  is the vector of state variables,  $y(t)$  is the output signal,  $u(t)$  is the input signal,  $f(x, u)$ ,  $h(x, u)$  are nonlinear functions. Then the nonlinear control system can be approximated to the linear control system according to the following formula:

$$\begin{aligned}\dot{x}(t) &= Ax(t) + Bu(t) \\ y(t) &= Cx(t) + Du(t)\end{aligned}\quad (23)$$

Where the matrices of the linear system at the equilibrium point are given by the following relations:

$$A = \left. \frac{\partial f(x, u)}{\partial x(t)} \right|_{(x_e, u_e)}, B = \left. \frac{\partial f(x, u)}{\partial u(t)} \right|_{(x_e, u_e)} \quad (24)$$

$$C = \left. \frac{\partial h(x, u)}{\partial x(t)} \right|_{(x_e, u_e)}, D = \left. \frac{\partial h(x, u)}{\partial u(t)} \right|_{(x_e, u_e)} \quad (25)$$

After finding the linear approximation of the unicycle robot system, the optimal linear quadratic controller is designed according to the following instructions:

```
clc;
clear all;
Ff=0;
Fa=0;
Frw=0;
Fpr=0;
AP = [0 1 0 0; 0 -192.3077*(Ff+Fa) 0 -9.0577+192.3077*Fa; 0 0 0 1; 0 1.4824 12.9155 -12.7944+13.4268*Ff+11.9444*Fa];
BP = [0; 192.3077; 0; -14.9091];
AW = [0 1 0 0; -94.7754 -5.6433*(Fpr+Frw) 0 5.6433; 0 0 1; 0 1587.3*Frw 0 -1587.3*Frw];
BW = [0; -5.6433; 0; 1587.3];
RP = 10;
QP = 10*eye(4);
[KP, SP, EP] = lqr(AP, BP, QP, RP);
RW = 10;
QW = 10*eye(4);
[KW, SW, EW] = lqr(AW, BW, QW, RW);
```

The first control beam is designed to regulate the robot arm and the second to regulate the robot wheel. After finding

the optimal control gains, they are applied to the nonlinear control system with the gain values being readjusted due to the nonlinearity of the single-wheel robot system.

## VII. DESIGN OF THE OPTIMAL PARAMETRIC QUADRATIC REGULATOR FOR THE UNICYCLE ROBOT SYSTEM [53]-[69]

An optimal parametric controller is defined as a control vector design for a control system that minimizes the performance function to a minimum value, taking into account the uncertainty of the control system parameters.

The optimal parametric controller is designed according to the following steps:

- First, the control statement must be formulated in affine form as follows:

$$\begin{aligned}\dot{x} &= \left\{ A_0 + \sum_{j=1}^N A_j \Delta_j \right\} x + B \cdot u \\ y &= C \cdot x\end{aligned}\quad (26)$$

Where as:

$$\Delta_j \in [-1, +1] \quad (27)$$

The linear and uncertain state equations are written according to formula (26), where ( $A_0$ ) is the nominal matrix, and the matrices ( $A_j$ ) are called uncertainty matrices.

- After finding the uncertainty matrices  $A_j$ , the matrices  $L_j$  and  $N_j$  are found as follows:

$$A_j = L_j N_j^T \quad (28)$$

- We find the matrices L and N from the previous matrices, as follows:

$$\begin{aligned}L &= [L_1 \ L_2 \ \dots \ L_j \ L_N] \\ N &= [N_1 \ N_2 \ \dots \ N_j \ N_N]\end{aligned}\quad (29)$$

- The optimal parametric control beam is given by the following formula:

$$u_{lqr}(t) = -K \cdot x(t) \quad (30)$$

- Where K is the optimal parametric control gain vector which is given by the following formula:

$$K = \frac{1}{\rho} R^{-1} B^T S \quad (31)$$

Where,  $\rho$  is a positive design parameter chosen randomly, and in the research it was chosen  $\rho_1 = 0.01$ ,  $\rho_2 = 0.01$  and it is calibrated randomly until the desired response is obtained. R is the weighting matrix given when choosing the performance function to be minimized, which has the following formula:

$$J = \int_0^\infty (x^T Q_0 x + u^T R u) dt \quad (32)$$

Where S is the solution of the following modified Riccati equation:

$$A_0^T S + S A_0^T - S \left( \frac{1}{\rho} B B^T - \frac{1}{\gamma} L L^T \right) S + Q_0 + \gamma N N^T = 0 \quad (33)$$

Where,  $\gamma$  is a positive design parameter chosen randomly, and is adjusted until the appropriate response is obtained, and in the research it was chosen  $\gamma_1 = 30, \gamma_2 = 3$ . The parameters  $(\rho, \gamma)$  are set randomly and there are no reliable leaders, but the adjustment is done until an acceptable solution is obtained. According to the scheme (8), the control signal is given by the difference between the reference signal  $r(t)$  and the linear combination consisting of the components of the state vector:

$$u(t) = r(t) - kx(t) \quad (34)$$

Where  $r(t)$  is the reference signal,  $k$  is the optimal parametric control gain vector of dimension  $(n)$  and where  $u(t)$  is the control vector that should be designed to minimize the cost function (28), both  $(Q, R)$  are positively defined symmetric matrices.

### VIII. APPLYING THE STEPS OF DESIGNING THE OPTIMAL PARAMETRIC QUADRATIC CONTROLLER TO THE UNI-WHEEL ROBOT SYSTEM [53]-[69]

To design the optimal parametric controller for the spherical robot system, we follow the following steps:

First: We represent the parameters of the friction factors in the following formula:

$$\mu_f \in [0.1, 0.7] \Rightarrow \mu_f = 0.4 + 0.3\delta_1 : \delta_1 \in [-1, +1] \quad (35)$$

$$\mu_a \in [0.1, 0.7] \Rightarrow \mu_a = 0.4 + 0.3\delta_2 : \delta_2 \in [-1, +1] \quad (36)$$

$$\mu_{pr} \in [0.1, 0.7] \Rightarrow \mu_{pr} = 0.4 + 0.3\delta_3 : \delta_3 \in [-1, +1] \quad (37)$$

$$\mu_{rw} \in [0.1, 0.7] \Rightarrow \mu_{rw} = 0.4 + 0.3\delta_4 : \delta_4 \in [-1, +1] \quad (38)$$

Second: We write the nonlinear state equations represented by formula (14) and (15) according to the affine formula represented by formula (26). The following instructions in the Matlab program show the programming of the optimal parametric controller according to the affine formula:

```

clc;
clear all;
Ff=0;
Fa=0;
Frw=0;
Fpr=0;
ro1=0.01;
gamma1=30;
A01=[0 1 0 0; 0 -153.8462 0 67.8654; 0.9 0 0 1; 0 1.4824
12.4824 -2.6459];
B1=[0; 192.3077; 0; -14.9091];
N1=[0 0; -7.5955 -7.5955; 0 0; 2.007 -0.4718]
L1=[0 0; 7.5955 7.5955; 0 0; 2.007 -7.5955]

```

```

B01 = (1/ro1)*B1*B1'-(1/gamma1)*L1*L1';
R1 = 1*eye(1);
Q1 = 0.01*eye(4);
C01 = Q1+gamma1*N1*N1';
P1 = are(A01, B01, C01);
KP1 = (1/ro1)*B1'*P1
ro2 = 0.01;
gamma2=3;
A02 = [0 1 0 0; -94.7354 -4.5146 0 5.6433; 0 0 0 1; 0
634.92 0 -634.92];
B2 = [0; -5.6433; 0; 1587.3];
N2 = [0 0; 1.3012 1.3012; 0 0; 0 365.9622];
L2 = [0 0; -1.3012 -1.3012; 0 0; 0 365.9622];
B02 = (1/ro2)*B2*B2'-(1/gamma2)*L2*L2';
R2 = 1*eye(1);
Q2 = 0.01*eye(4);
C02 = Q2+gamma2*N2*N2';
P2 = are(A02,B02,C02);
KP2 = (1/ro2)*B2'*P2

```

By designing the optimal parametric regulator and simulating it using Matlab and designing the diagram using (Simulink) which represents the nonlinear unicycle robot system with the optimal parametric regulator, we get the diagram [44]-[51].

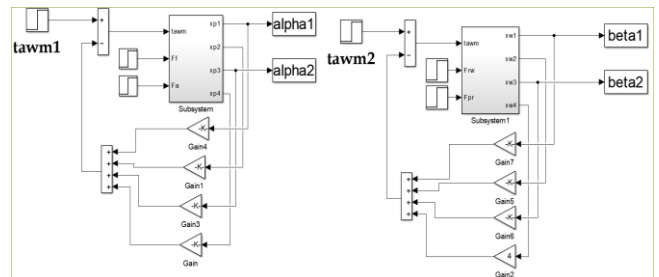


Fig. 9. The unicycle robot assembly with the optimal parametric controller

- Robot arm angle response  $\alpha_1(t)$ :

Shown in Fig. 10 Robot arm angle response  $\alpha_1(t)$ , for zero friction factors.

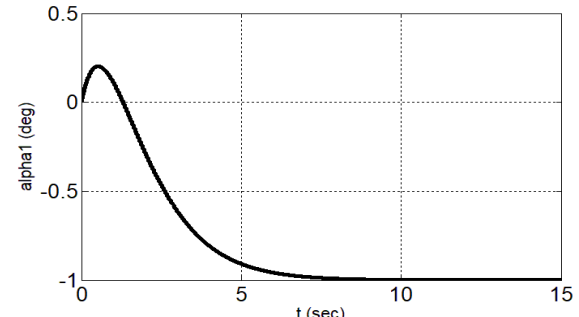


Fig. 10. Robot arm angle response  $\alpha_1(t)$  for zero friction factors

- Roll Angle Response of Robot Arm  $\alpha_2(t)$ :

Roll Angle Response of Robot Arm shown in Fig. 11, for zero friction factors.

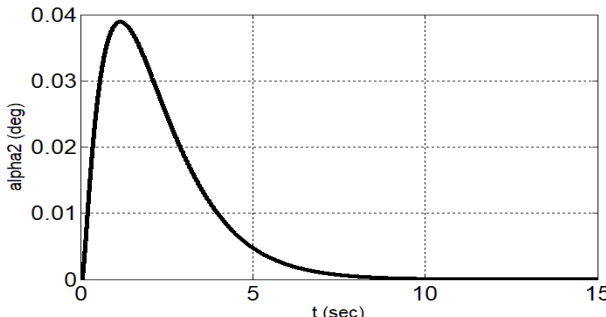


Fig. 11. Roll angle response of robot arm  $\alpha_2(t)$  for zero friction factors

- The angular response resulting from the wheel rotation relative to the vertical line  $\beta_1(t)$ :

Shown in Fig. 12 Robot wheel rotation angle response to vertical line  $\beta_1(t)$ , for zero friction factors.

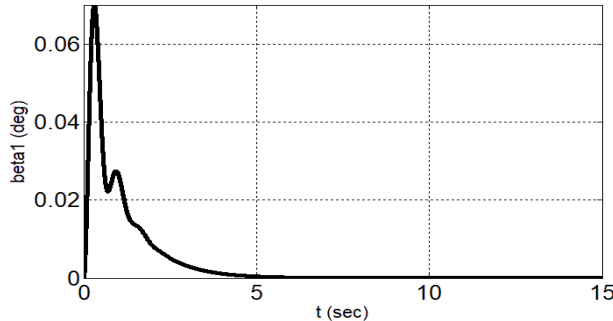


Fig. 12. The response of the robot wheel rotation angle to the plumb line  $\beta_1(t)$  for zero friction factors.

- Angle response resulting from wheel rotation  $\beta_2(t)$ :

When applying the optimal controller to the nonlinear single-wheel robot system, we obtain the angular response resulting from the rotation of the wheel and the axis perpendicular to the wheel plane  $\beta_2(t)$  shown in Fig. 13, for zero friction factors.

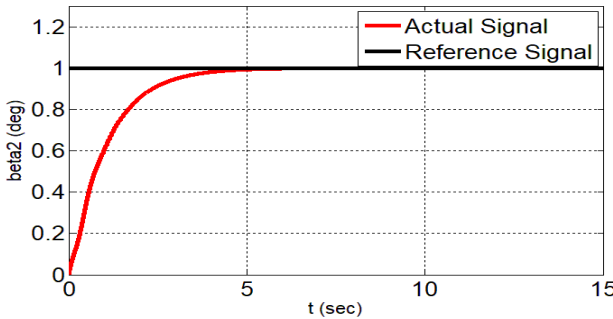


Fig. 13. The angle response resulting from wheel rotation  $\beta_2(t)$  for zero friction factors

#### A. Analysis of the Response Results when using the Optimal Controller without Friction Factors

From Fig. 13, we notice that the wheel rotation angle was followed by the unitary reference signal according to an inertial response, and therefore the arm must then react in

reverse, and therefore to restore the balance of the robot arm, the response must be at a negative angle. This is shown in Fig. 10, where the arm angle follows the unitary signal, but with a negative value to counteract the wheel angle and achieve balance. We notice at the beginning of the transient state the presence of a positive peak for the angle, and this peak indicates the movement of the arm at the beginning of take-off in the same direction as the wheel angle, and then it returns to the negative value to achieve balance.

We note that both angular responses  $\alpha_2(t)$  and  $\beta_1(t)$  return to zero, indicating that equilibrium is achieved. Thus, we note the success of the optimal controller in achieving the wheel's pursuit of the reference signal and achieving the balance of the robot arm in the vertical position when there are no friction factors.

#### B. Response of the Arm of the Single-Wheel Robot in the Presence of Friction Factors

Friction factors arise between the point of contact of the robot's wheel and the ground due to the roughness of the ground on which the single-wheel robot moves, so the response of the single-wheel robot was studied for several friction factors, and the following responses were obtained:

- Robot arm angle response  $\alpha_1(t)$ :

Fig. 14 shows the Robot arm angle response  $\alpha_1(t)$ , for several friction factors.

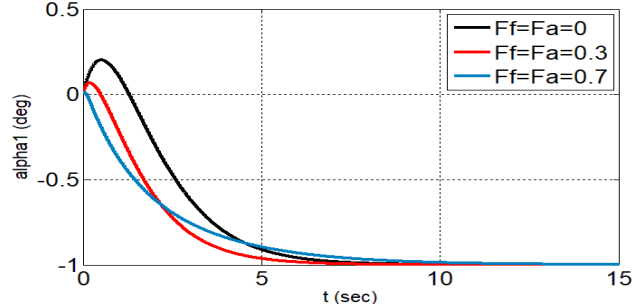


Fig. 14. Robot arm angle response  $\alpha_1(t)$  for various friction factors

- Roll Angle Response of Robot Arm  $\alpha_2(t)$ :

Fig. 15 shows the Roll Angle Response of Robot Arm  $\alpha_2(t)$ , for several friction factors.

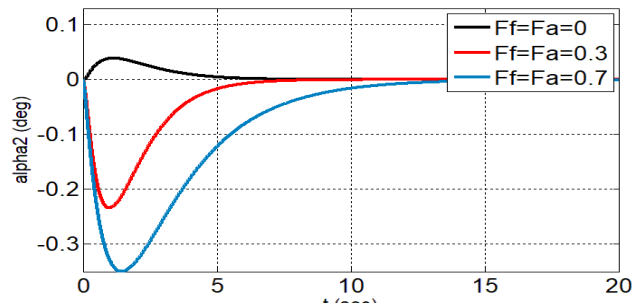


Fig. 15. Roll angle response of robot arm  $\alpha_2(t)$  for various friction factors

- The angular response resulting from the wheel rotation angle relative to the vertical line  $\beta_1(t)$ :

Shown in Fig. 16 Robot wheel rotation response to vertical line  $\beta_1(t)$ , for several friction factors.

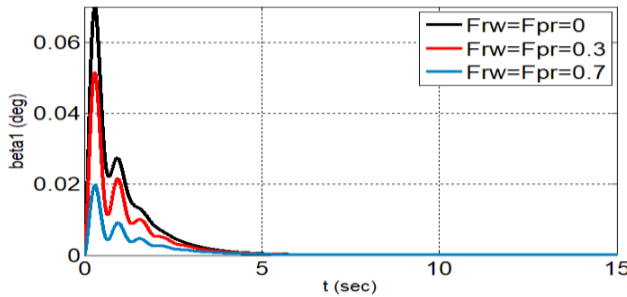


Fig. 16. The response of the robot wheel rotation angle to the plumb line  $\beta_1(t)$  for several friction factors

- Angle response resulting from wheel rotation  $\beta_2(t)$ :

Fig. 17 shows the Angle response resulting from wheel rotation  $\beta_2(t)$ , for several friction factors.

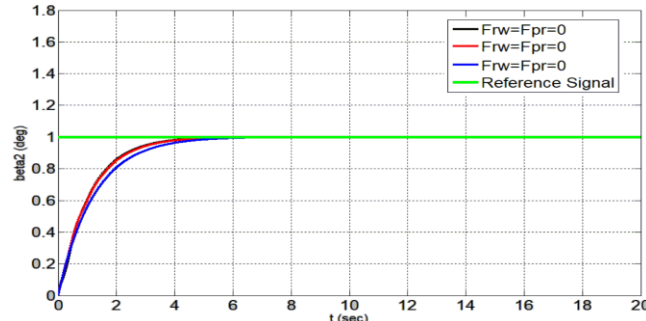


Fig. 17. The Angle response resulting from wheel rotation  $\beta_2(t)$  for several friction factors

### C. Analysis of the Response Results when using the Optimal Controller for Multiple Friction Factors

Through the previous figures from Fig. 14 to Fig. 17, we notice the success of the linear quadratic optimal controller in achieving the stability of the single-wheel robot system for multiple friction values, and even that stability remains achieved at very large friction values of order (0.7). Therefore, the nonlinear single-wheel robot maintains its performance well when moving on rough and smooth surfaces, with very small time differences.

In this paragraph, the mechanism for designing the linear quadratic optimal controller is explained, after representing the control set in the form of affine.

### IX. WHEN APPLYING THE OPTIMAL PARAMETRIC CONTROLLER

The proposed system was simulated using the MATLAB/Simulink environment and the performance of the optimal parametric controller was tested for multiple friction factors, as follows:

#### A. Response of the Arm of the Single-Wheel Robot System without Friction Factors

For zero friction factors, the following responses were obtained:

- Robot arm angle response  $\alpha_1(t)$ :

Fig. 18 shows the Robot arm angle response  $\alpha_1(t)$ , for zero friction factors.

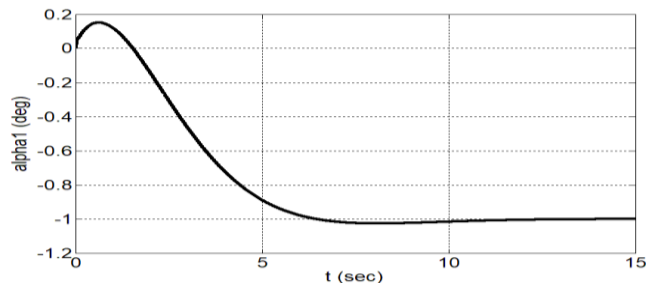


Fig. 18. Robot arm angle response  $\alpha_1(t)$  for zero friction factors

- Roll Angle Response of Robot Arm  $\alpha_2(t)$ :

Fig. 19 shows the Roll Angle Response of Robot Arm  $\alpha_2(t)$ , for zero friction factors.

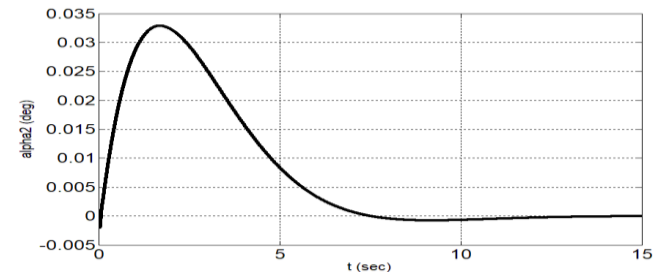


Fig. 19. Roll angle response of robot arm  $\alpha_2(t)$  for zero friction factors

- The angular response resulting from the wheel rotation angle relative to the vertical line  $\beta_1(t)$ :

Shown in Fig. 20 Robot wheel rotation response to vertical line  $\beta_1(t)$ , for zero friction factors.

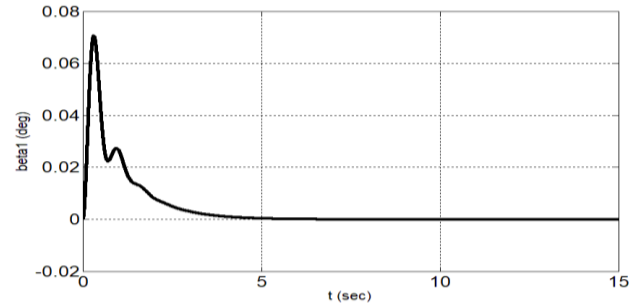


Fig. 20. The response of the robot wheel rotation angle to the plumb line  $\beta_1(t)$  for zero friction factors

- Angle response resulting from wheel rotation  $\beta_2(t)$ :

Fig. 21 shows the Angle response resulting from wheel rotation  $\beta_2(t)$ , for zero friction factors.

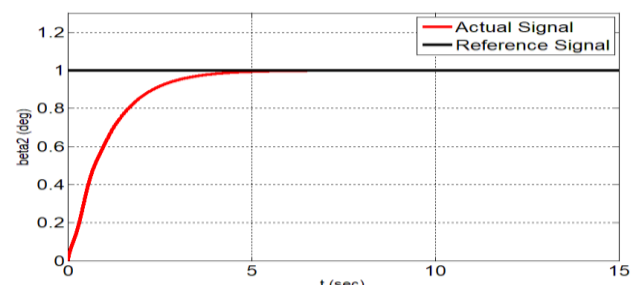


Fig. 21. The angle response resulting from wheel rotation  $\beta_2(t)$  for zero friction factors

### B. Analysis of the Response Results when using the Optimal Parametric Controller without Friction Factors:

From Fig. 21, we notice that the wheel rotation angle was followed by the reference signal according to an inertial response, and therefore the arm must react in reverse, and therefore to restore the balance of the robot arm, the response must be at a negative angle, and this is shown in Fig. 18, where the arm angle follows the reference signal but with a negative value to counteract the wheel angle and achieve balance, and we notice at the beginning of the transient state the presence of a positive peak for the angle, and this peak indicates the movement of the arm at the beginning of take-off in the same direction as the wheel angle, and then it returns to the negative value to achieve balance. We notice that both angular responses  $\alpha_2(t)$  and  $\beta_1(t)$  return to zero, which indicates that balance has been achieved. Thus, we notice the success of the optimal parametric controller in achieving the wheel's pursuit of the reference signal and achieving the balance of the robot arm in the vertical position when there are no friction factors.

### C. Comparison of the Responses of the Optimal and Optimal Parametric Controllers in the Presence of Friction Factors:

The responses resulting from the design of the optimal and optimal parametric controllers will be compared for different friction factors, as friction factors arise between the contact point of the robot wheel and the ground according to the roughness of the ground on which the single-wheeled robot moves, so the response of the single-wheeled robot was studied for several friction factors.

First: For friction factors  $Ff = Fa = 0.3$ ,  $Frw = Fpr = 0.3$ :

- Comparison of the Robot arm angle response  $\alpha_1(t)$ :

Fig. 22 shows the Robot arm angle response  $\alpha_1(t)$ , for friction factors:  $Ff = Fa = 0.3$ :

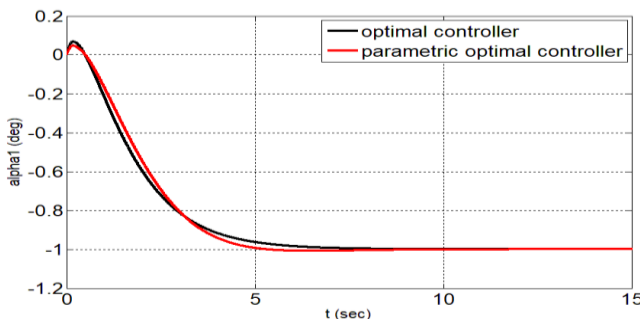


Fig. 22. Comparison of the response of angle  $\alpha_1(t)$  when using the optimal and optimal parametric controllers for friction factors  $Ff = Fa = 0.3$

- Roll Angle Response of Robot Arm  $\alpha_2(t)$ :

Fig. 23 shows Roll Angle Response of Robot Arm  $\alpha_2(t)$ , for friction factors:  $Ff = Fa = 0.3$ .

- The angular response resulting from the wheel rotation relative to the vertical line  $\beta_1(t)$ :

Shown in Fig. 24 Robot wheel rotation angle response to vertical line  $\beta_1(t)$ , for friction factors:  $Frw = Fpr = 0.3$ .

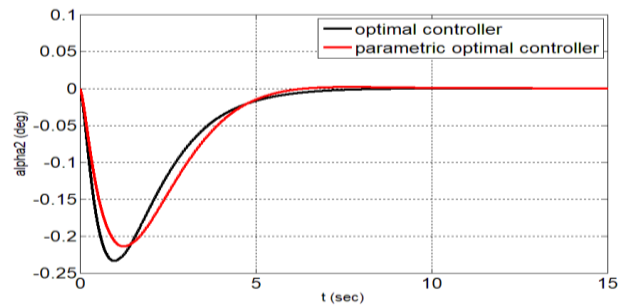


Fig. 23. Comparison of roll angle response of robot arm  $\alpha_2(t)$  when using the optimal and optimal parametric controllers for friction factors  $Ff = Fa = 0.3$

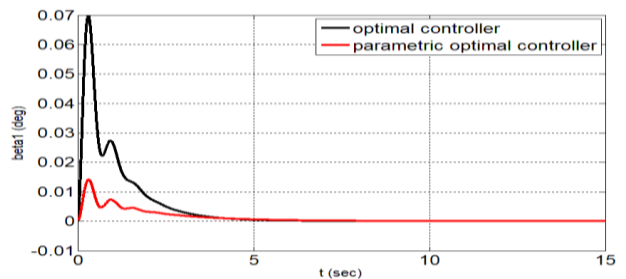


Fig. 24. Comparison of the response of the angle  $\beta_1(t)$  when using the optimal and optimal parametric controllers for friction factors  $Frw = Fpr = 0.3$

- Angle response resulting from wheel rotation  $\beta_2(t)$ :

Fig. 25 shows the Angle response resulting from wheel rotation  $\beta_2(t)$ , for friction factors:  $Frw = Fpr = 0.3$

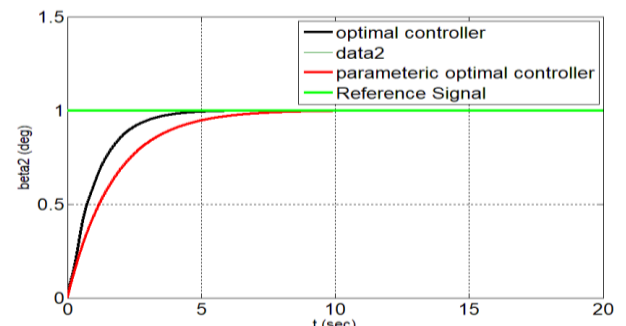


Fig. 25. Comparison of the response of angle  $\beta_2(t)$  when using the optimal and optimal parametric controllers for friction factors  $Frw = Fpr = 0.3$

- Comparison of the Robot arm angle response  $\alpha_1(t)$ :

Fig. 26 shows the Robot arm angle response  $\alpha_1(t)$ , for friction factors:  $Ff = Fa = 0.7$

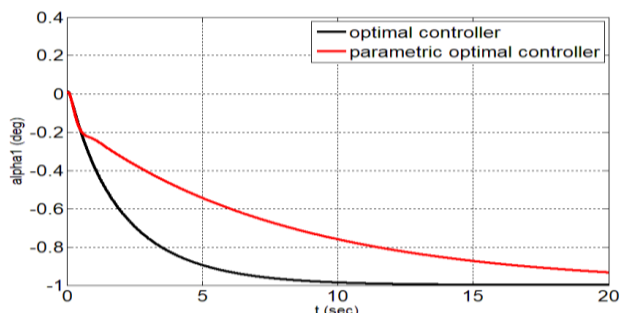


Fig. 26. Comparison of the response of angle  $\alpha_1(t)$  when using the optimal and optimal parametric controllers for friction factors  $Ff = Fa = 0.7$

- Roll Angle Response of Robot Arm  $\alpha_2(t)$ :

Fig. 27 shows the response Roll Angle Response of Robot Arm  $\alpha_2(t)$ , for friction factors:  $Ff = Fa = 0.7$

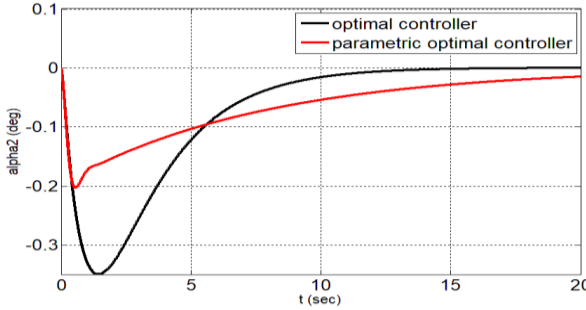


Fig. 27. Comparison of the Roll Angle Response of Robot Arm  $\alpha_2(t)$  when using the optimal and optimal parametric controllers for friction factors  $Ff = Fa = 0.7$

- The angular response resulting from the wheel rotation angle relative to the vertical line  $\beta_1(t)$ :

Shown in Fig. 28 Robot wheel rotation response to vertical line  $\beta_1(t)$ , for friction factors:  $Frw = Fpr = 0.7$

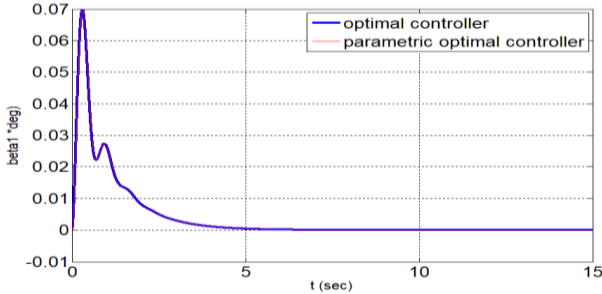


Fig. 28. Comparison of the response of angle  $\beta_1(t)$  when using the optimal and optimal parametric controllers for friction factors  $Frw = Fpr = 0.7$

- Angle response resulting from wheel rotation  $\beta_2(t)$ :

Fig. 29 shows the Angle response resulting from wheel rotation  $\beta_2(t)$ , for friction factors:  $Frw = Fpr = 0.7$

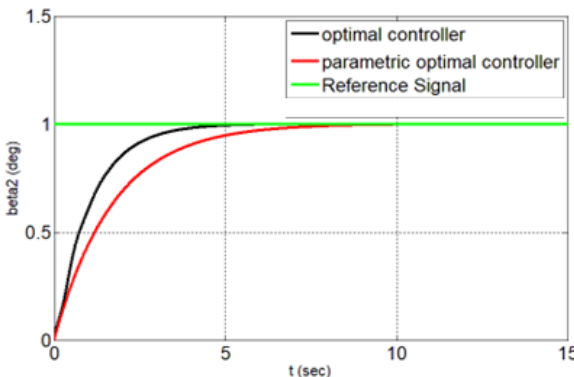


Fig. 29. Comparison of the response of angle  $\beta_2(t)$  when using the optimal and optimal parametric controllers for friction factors  $Frw = Fpr = 0.7$

## X. ANALYSIS OF THE RESPONSE RESULTS WHEN USING OPTIMAL AND PARAMETRIC OPTIMAL CONTROLLERS FOR VARIOUS FRICTION FACTORS

Through the response forms shown in Fig. 22 to Fig. 28 above, we notice the success of the optimal linear quadratic controller and the optimal parametric regulator in achieving

the stability of the single-wheel robot system for many friction values, and even that stability remains achieved at very large friction values of order (0.7). Therefore, the nonlinear single-wheel robot maintains its performance well when moving on rough and smooth surfaces, with very small time differences. It can be noted that the optimal parametric controller outperforms the optimal controller in general. According to Fig. 22 and Fig. 23, we notice that in the transient state stage, the optimal parametric controller outperforms, and according to Fig. 24, we notice that the maximum overshoot when applying the optimal parametric controller is much better than the optimal controller.

Table III shows a summary of the temporal features as a result of comparing the two controllers for the factors  $Ff = Fa = 0.3, Frw = Fpr = 0.3$ .

TABLE III. SHOWS A SUMMARY OF THE TEMPORAL FEATURES AS A RESULT OF THE COMPARISON BETWEEN THE TWO CONTROLLERS FOR THE FOLLOWING FACTORS  $Ff = Fa = 0.3, Frw = Fpr = 0.3$

$Ff = Fa = 0.3$ $Frw = Fpr = 0.3$				
Optimal Parametric Controller		linear quadratic optimal controller		applied controller
$\beta_2(t)$	$\alpha_1(t)$	$\beta_2(t)$	$\alpha_1(t)$	
$T_r = 1.704 \text{ sec}$	$T_r = 2.3 \text{ sec}$	$T_r = 1.064 \text{ sec}$	$T_r = 2.14 \text{ sec}$	Rise Time
$T_s = 6.695 \text{ sec}$	$T_s = 4.658 \text{ sec}$	$T_s = 3.975 \text{ sec}$	$T_s = 5.78 \text{ sec}$	Stability time
Non	$M_p = 4.765 \text{ } \%_0$	Non	$M_p = 6.85 \text{ } \%_0$	Maximum overshoot
Non	$T_p = 0.2 \text{ sec}$	Non	$T_p = 0.2 \text{ sec}$	Maximum overshoot time

Table IV shows the summary of the temporal features as a result of the comparison between the two controllers for the factors  $Ff = Fa = 0.7, Frw = Fpr = 0.7$ .

TABLE IV. SHOWS THE SUMMARY OF THE TEMPORAL FEATURES AS A RESULT OF THE COMPARISON BETWEEN THE TWO CONTROLLERS FOR THE FACTORS  $Ff = Fa = 0.7, Frw = Fpr = 0.7$

$Ff = Fa = 0.7$ $Frw = Fpr = 0.7$				
Optimal Parametric Controller		linear quadratic optimal controller		applied controller
$\beta_2(t)$	$\alpha_1(t)$	$\beta_2(t)$	$\alpha_1(t)$	
$T_r = 1.705 \text{ sec}$	$T_r = 6.66 \text{ sec}$	$T_r = 1.064 \text{ sec}$	$T_r = 2.105 \text{ sec}$	Rise Time
$T_s = 6.695 \text{ sec}$	$T_s > 10 \text{ sec}$	$T_s = 3.97 \text{ sec}$	$T_s = 9.06 \text{ sec}$	Stability time
Non	Non	Non	Non	Maximum overshoot
Non	Non	Non	Non	Maximum overshoot time

When designing the optimal parametric controller, the uncertainty of the friction factors was taken into consideration because the uni-wheeled robot's sentence was not written in affine form. As for the linear quadratic optimal controller, it was designed at the nominal values of the friction factors. This justifies the superiority of the optimal parametric controller over the optimal controller sometimes, and at other times the superiority of the linear quadratic optimal controller over the optimal parametric controller,

depending on the distance of the friction factor values from the nominal values.

The research can be developed by taking into account non-meteoric terrain, as well as variable friction coefficients, avoiding obstacles that may obstruct the path of the single-wheel robot, and adaptive controllers can be used and their results compared with the research results.

## REFERENCES

- [1] H. Ríos, M. Mera, T. Raïssi, and D. Efimov, "An Integral Sliding-Mode-Based Robust Interval Predictive Control for Perturbed Unicycle Mobile Robots," *2023 62nd IEEE Conference on Decision and Control (CDC)*, pp. 6978–6983, 2023, doi: 10.1109/CDC49753.2023.10383445.
- [2] J. A. Roteta Lannes and A. G. García, "Unicycle Robot's Navigation Control with Obstacle Avoidance and Asymptotic Stability," *American Journal of Engineering and Applied Sciences*, vol. 17, no. 1, pp. 40–45, 2024.
- [3] A. G. García, "Asymptotic stability of unicycle-like robots: The Bessel's controller," *Journal of Mechatronics and Robotics*, vol. 4, no. 1, pp. 1–7, 2020, doi: 10.3844/jmrsp.2020.
- [4] A. İslelen, N. van de Wouw, and Ö. Arslan, "Feedback Motion Prediction for Safe Unicycle Robot Navigation," *2023 IEEE/RSJ International Conference on Intelligent Robots and Systems (IROS)*, pp. 10511–10518, 2023, doi: 10.1109/IROS55552.2023.10341787.
- [5] P. Rochel, H. Ríos, M. Mera, and A. Dzul, "Trajectory tracking for uncertain Unicycle Mobile Robots: A Super-Twisting approach," *Control Engineering Practice*, vol. 122, p. 105078, 2022.
- [6] J. Huang, "Research and design of unicycle robot based on cascade PID control," in *International Conference on Mechatronic Engineering and Artificial Intelligence (MEAII 2023)*, vol. 13071, pp. 795–803, 2024.
- [7] Z. Sun, L. Dai, and K. Johansson, "Robust MPC for tracking constrained unicycle robots with additive disturbances," *Automatica*, vol. 90, pp. 172–184, 2018.
- [8] A. Rahmanian, A. A. Nasab, and M. H. Asemani, "A Control Barrier Function Based Approach for Safe and Efficient Navigation of Unicycle Mobile Robots," *2024 10th International Conference on Control, Instrumentation and Automation (ICCIA)*, pp. 1–6, 2024, doi: 10.1109/ICCIA65044.2024.10768176.
- [9] X. Cao, D. C. Bui, D. Takács, and G. Orosz, "Autonomous unicycle: modeling, dynamics, and control," *Multibody System Dynamics*, vol. 61, no. 1, pp. 43–76, 2024.
- [10] W. B. Qin, Y. Zhang, D. Takács, G. Stépán, and G. Orosz, "Nonholonomic dynamics and control of road vehicles: moving toward automation," *Nonlinear Dynamics*, vol. 110, no. 3, pp. 1959–2004, 2022.
- [11] Q. Cao, Z. Sun, Y. Xia, and L. Dai, "Self-triggered MPC for trajectory tracking of unicycle-type robots with external disturbance," *Journal of the Franklin Institute*, vol. 356, no. 11, pp. 5593–5610, 2019.
- [12] H. Xiao et al., "Robust Stabilization of a Wheeled Mobile Robot Using Model Predictive Control Based on Neurodynamics Optimization," in *IEEE Transactions on Industrial Electronics*, vol. 64, no. 1, pp. 505–516, Jan. 2017, doi: 10.1109/TIE.2016.2606358.
- [13] Z. Sun, L. Dai, K. Liu, Y. Xia, and K. Johansson, "Robust MPC for tracking constrained unicycle robots with additive disturbances," *Automatica*, vol. 90, pp. 172–184, 2018.
- [14] Z. Sun, Y. Xia, L. Dai, and P. Campoy, "Tracking of unicycle robots using event-based MPC with adaptive prediction horizon," *IEEE/ASME Transactions on Mechatronics*, vol. 25, no. 2, pp. 739–749, 2020.
- [15] D. Vos and A. Von Flotow, "Dynamics and nonlinear adaptive control of an autonomous unicycle: theory and experiment," in *Proc. 29th IEEE Conf. Decision and Control*, pp. 182–187, 1990.
- [16] J. P. Meijaard, J. M. Papadopoulos, A. Ruina, and A. L. Schwab, "Linearized dynamics equations for the balance and steer of a bicycle: a benchmark and review," *Proc. R. Soc. A*, vol. 463, no. 2084, pp. 1955–1982, 2007.
- [17] Y. Naveh, P. Bar Yoseph, and Y. Halevi, "Nonlinear modeling and control of a unicycle," *Dyn. Control*, vol. 9, pp. 279–296, 1999.
- [18] B. Pollard, V. Fedonyuk, and P. Tallapragada, "Swimming on limit cycles with nonholonomic constraints," *Nonlinear Dyn.*, vol. 97, no. 4, pp. 2453–2468, 2019.
- [19] X. Ruan, J. Hu, and Q. Wang, "Modeling with Euler-Lagrange equation and cybernetical analysis for a unicycle robot," in *Proc. 2nd Int. Conf. Intelligent Computation Technology and Automation*, pp. 108–111, 2009.
- [20] A. Schoonwinkel. *Design and test of a computer stabilized unicycle*. Stanford University, 1987.
- [21] Z. Sheng and K. Yamafuji, "Study on the stability and motion control of a unicycle: part I: dynamics of a human riding a unicycle and its modeling by link mechanisms," *JSME Int. J. Ser. C*, vol. 38, no. 2, pp. 249–259, 1995.
- [22] H. Suzuki, S. Moromugi, and Okura, "Development of robotic unicycles," *J. Robot. Mechatron.*, vol. 26, no. 5, pp. 540–549, 2014.
- [23] L. Consolini, F. Morbidi, D. Prattichizzo, and M. Tosques, "Leader-follower formation control of nonholonomic mobile robots with input constraints," *Automatica*, vol. 44, no. 5, pp. 1343–1349, 2008.
- [24] D. Gu and H. Hu, "Receding horizon tracking control of wheeled mobile robots," *IEEE Trans. Control Syst. Technol.*, vol. 14, no. 4, pp. 743–749, 2006.
- [25] J. A. Marshall, M. E. Broucke, and B. A. Francis, "Pursuit formations of unicycles," *Automatica*, vol. 42, no. 1, pp. 3–12, 2006.
- [26] Z. Lin, B. Francis, and M. Maggiore, "Necessary and sufficient graphical conditions for formation control of unicycles," *IEEE Trans. Autom. Control*, vol. 50, no. 1, pp. 121–127, 2005.
- [27] Z. Sun and Y. Xia, "Receding horizon tracking control of unicycle-type robots based on virtual structure," *Int. J. Robust Nonlinear Control*, vol. 26, no. 17, pp. 3900–3918, 2016.
- [28] D. Zenkov, A. Bloch, and J. Marsden, "The Lyapunov-Malkin theorem and stabilization of the unicycle with rider," *Syst. Control Lett.*, vol. 45, pp. 293–300, 2002.
- [29] A. G. García, "Asymptotic stability of unicycle-like robots: The Bessel's controller," *Journal of Mechatronics and Robotics*, vol. 4, no. 1, pp. 1–7, 2020, doi: 10.3844/jmrsp.2020.1.7.
- [30] D. Kostić, S. Adinandra, J. Caarls, N. van de Wouw, and H. Nijmeijer, "Collision-free tracking control of unicycle mobile robots," in *Proc. 48th IEEE Conf. Decision and Control (CDC) Held Jointly with 2009 28th Chinese Control Conf.*, pp. 5667–5672, 2009, doi: 10.1109/CDC.2009.5400088.
- [31] M. Nielačzny, W. Bies, and T. Kapitaniak. *Dynamics of the Unicycle: Modelling and Experimental Verification*. Springer International Publishing, 2019.
- [32] Y. Isomi and S. Majima, "Tracking control method for an underactuated unicycle robot using an equilibrium state," in *Proc. 2009 IEEE Int. Conf. Control and Automation*, pp. 1844–1849, 2009.
- [33] J. I. Neimark and N. A. Fufaev, "Dynamics of Nonholonomic Systems," *Translations of Mathematical Monographs*, vol. 33, 1972.
- [34] S. Ostrovskaia and J. Angeles, "Nonholonomic systems revisited within the framework of analytical mechanics," *Appl. Mech. Rev.*, vol. 57, no. 7, pp. 415–433, 1998.
- [35] J. G. Papastavridis. *Analytical Mechanics*. World Scientific, 2002.
- [36] G. P. Incremona, A. Ferrara, and L. Magni, "Asynchronous networked MPC with ISM for uncertain nonlinear systems," *IEEE Transactions on Automatic Control*, vol. 62, no. 9, pp. 4305–4317, 2017.
- [37] M. Rubagotti, G. P. Incremona, D. M. Raimondo, and A. Ferrara, "Constrained nonlinear discrete-time sliding mode control based on a receding horizon approach," *IEEE Transactions on Automatic Control*, vol. 66, no. 8, pp. 3802–3809, 2021.
- [38] M. Guerra, D. Efimov, G. Zheng, and W. Perruquetti, "Avoiding local minima in the potential field method using input-to-state stability," *Control Engineering Practice*, vol. 55, pp. 174–184, 2016.
- [39] V. Utkin, J. Guldner, and J. Shi. *Sliding Modes in Electromechanical Systems*. London: Taylor and Francis, 1999.
- [40] F. Castaños and L. Fridman, "Analysis and design of integral sliding manifolds for systems with unmatched perturbations," *IEEE Transactions on Automatic Control*, vol. 51, no. 5, pp. 853–858, 2006.
- [41] C. Rodwell and P. Tallapragada, "Induced and tunable multistability due to nonholonomic constraints," *Nonlinear Dyn.*, vol. 108, no. 3, pp. 2115–2126, 2022.

- [42] D. Efimov, W. Perruquetti, T. Raïssi, and A. Zolghadri, "Interval observers for time-varying discrete-time systems," *IEEE Transactions on Automatic Control*, vol. 58, no. 12, pp. 3218–3224, 2013.
- [43] D. Efimov, T. Raïssi, and A. Zolghadri, "Control of nonlinear and LPV systems: Interval observer-based framework," *IEEE Transactions on Automatic Control*, vol. 58, no. 3, pp. 773–778, 2013.
- [44] B. Várszegi, D. Takács, and G. Orosz, "On the nonlinear dynamics of automated vehicles – a nonholonomic approach," *Eur. J. Mech. A, Solids*, vol. 74, pp. 371–380, 2019.
- [45] P. Appell, "Sur une forme générale des équations de la dynamique (On a general form of the equations of dynamics)," *J. Reine Angew. Math.*, vol. 121, pp. 310–319, 1900.
- [46] H. Baruh. *Analytical Dynamics*. New York: McGraw-Hill, 1999.
- [47] A. M. Bloch. *Nonholonomic Mechanics and Control*. Berlin: Springer, 2003.
- [48] A. De Luca, G. Oriolo, and C. Samson, "Feedback control of a nonholonomic car-like robot," in *Robot Motion Planning and Control*, pp. 171–249, 1998.
- [49] E. Desloge, "A comparison of Kane's equations of motion and the Gibbs–Appell equations of motion," *Am. J. Phys.*, vol. 54, pp. 470–472, 1986.
- [50] E. Desloge, "Relationship between Kane's equations and the Gibbs–Appell equations," *J. Guid. Control Dyn.*, vol. 10, pp. 120–1222, 1987.
- [51] E. Desloge, "The Gibbs–Appell equations of motion," *Am. J. Phys.*, vol. 56, pp. 841–846, 1988.
- [52] F. Gantmacher. *Lectures in Analytical Mechanics*. Moscow: MIR Publishers, 1970
- [53] J. W. Gibbs, "On the fundamental formulae of dynamics," *Am. J. Math.*, vol. 2, no. 1, pp. 49–64, 1879.
- [54] D. T. Greenwood. *Advanced Dynamics*. Cambridge: Cambridge University Press, 2003.
- [55] O. Halvani and Y. Or, "Nonholonomic dynamics of the twistcar vehicle: asymptotic analysis and hybrid dynamics of frictional skidding," *Nonlinear Dyn.*, vol. 107, no. 3, pp. 3443–3459, 2022.
- [56] G. Hamel, "Nichtholome Systeme höherer Art (Nonholonomic systems of a higher kind)," *Sitzungsber. Berl. Math. Ges.*, vol. 37, pp. 41–52, 1938.
- [57] H. Z. Horvath and D. Takács, "Control design for balancing a motorbike at zero longitudinal speed," in *Proc. 15th Int. Symp. Advanced Vehicle Control*, 2022.
- [58] T. R. Kane, "Dynamics of nonholonomic systems," *J. Appl. Mech.*, vol. 28, pp. 574–578, 1961.
- [59] T. Kane, "Rebuttal to 'A comparison of Kane's equations of motion and the Gibbs–Appell equations of motion'," *Am. J. Phys.*, vol. 54, pp. 472, 1986.
- [60] T. R. Kane and D. A. Levinson. *Dynamics, Theory and Applications*. New York: McGraw-Hill, 1985.
- [61] W. S. Koon and J. E. Marsden, "The Hamiltonian and Lagrangian approaches to the dynamics of nonholonomic systems," *Rep. Math. Phys.*, vol. 40, no. 1, pp. 21–62, 1997.
- [62] W. B. Qin, Y. Zhang, D. Takács, and G. Orosz, "Nonholonomic dynamics and control of road vehicles: moving toward automation," *Nonlinear Dyn.*, vol. 110, no. 3, pp. 1959–2004, 2022.
- [63] J. Yang, Y. Zhao, X. Liu, and L. Zhang, "Optimal Planning and Control of Robots," Submission deadline: Sunday, 31 March 2024.
- [64] J. Berner, L. Richter, and K. Ullrich, "An optimal control perspective on diffusion-based generative modeling," *arXiv preprint arXiv:2211.01364*, 2022.
- [65] Y. Kumar, P. V. Chanekar, and S. B. Roy, "Optimal Observer-Based Controller Design for Linear Systems," *2024 European Control Conference (ECC)*, pp. 1380-1386, 2024, doi: 10.23919/ECC64448.2024.10590735.
- [66] E. J. Routh. *The Advanced Part of a Treatise on the Dynamics of a System of Rigid Bodies*. London: Macmillan & Co., 1884.
- [67] G. Teschl. *Ordinary Differential Equations and Dynamical Systems*. Providence: Am. Math. Soc., 2012.
- [68] A. Voss, "Ueber die Differential gleichungen der Mechanik", *Math. Ann.*, vol. 25, pp. 258–286, 1885.
- [69] T. Yona and Y. Or, "The wheeled three-link snake model: singularities in nonholonomic constraints and stick-slip hybrid dynamics induced by Coulomb friction," *Nonlinear Dyn.*, vol. 95, no. 3, pp. 2307–2324, 2019.
- [70] K. Kimura, K. Ogata, and K. Ishii, "Novel Mathematical Modeling and Motion Analysis of a Sphere Considering Slipping," *Journal of Robotics, Networking and Artificial Life*, vol. 6, no. 1, June 2019.
- [71] G. Terekhov and V. Pavlovsky, "Controlling spherical mobile robot in a two-parametric friction model," *MATEC Web of Conferences*, vol. 113, p. 02007, 2017.
- [72] D. Zunt. *Who did actually invent the word "robot" and what does it mean?*. The Karel Čapek website, 2005.
- [73] E. Falotico *et al.*, "Connecting artificial brains to robots in a comprehensive simulation framework: the neurorobotics platform," *Frontiers in neurorobotics*, vol. 11, 2017.
- [74] V. De Sario. *Advanced Analytical Dynamics: Theory and Applications*. Cambridge: Cambridge University Press, 2017.
- [75] J. Schwartz, "In the Lab: Robots That Slink and Squirm," *The New York Times: Science*, pp. 1-4, 2007.
- [76] C. Manceaux-Cumer. *Techiques de Commande Robust*. Ecole nationale supérieure de l'aéronautique et de l'espace, version provisoire, 1998.
- [77] Y. Ming, D. Zongquan, Y. Xinyi, and Y. Weizhen, "Introducing HIT Spherical Robot: Dynamic Modeling and Analysis Based on Decoupled Subsystem," in *Proc. 2006 IEEE Int. Conf. Robotics and Biomimetics*, pp. 181–186, 2006.
- [78] M. Steinberger, I. Castillo, M. Horn, and L. Fridman, "Robust output tracking of constrained perturbed linear systems via model predictive sliding mode control," *International Journal of Robust and Nonlinear Control*, vol. 30, no. 3, pp. 1258–1274, 2020.
- [79] R. Galván-Guerra, G. P. Incremona, L. Fridman, and A. Ferrara, "Robust multi-model predictive control via integral sliding modes," *IEEE Control Systems Letters*, vol. 6, pp. 2623–2628, 2022.
- [80] A. dos Reis de Souza, D. Efimov, and T. Raïssi, "Robust output feedback MPC for LPV systems using interval observers," *IEEE Transactions on Automatic Control*, vol. 67, no. 6, pp. 3188–3195, 2022.